Ain Shams Engineering Journal (2014) 5, 293–304

Ain Shams University

Ain Shams Engineering Journal

www.elsevier.com/locate/asej
www.sciencedirect.com

ENGINEERING PHYSICS AND MATHEMATICS

Series solution of unsteady peristaltic flow of a Carreau fluid in eccentric cylinders

S. Nadeem [a], Arshad Riaz [b,*], R. Ellahi [b,c], Noreen Sher Akbar [d]

[a] Department of Mathematics, Quaid-i-Azam University 45320, Islamabad 44000, Pakistan
[b] Department of Mathematics and Statistics, FBAS, IIU, Islamabad 44000, Pakistan
[c] Department of Mechanical Engineering, Bourns Hall A 373, University of California, Riverside, CA 92521, USA
[d] DBS&H, CEME, National University of Sciences and Technology, Islamabad, Pakistan

Received 19 June 2013; revised 30 August 2013; accepted 9 September 2013
Available online 15 November 2013

KEYWORDS

Peristaltic flow;
Eccentric cylinders;
Carreau fluid;
Analytical series solution

Abstract In the present analysis, the unsteady peristaltic flow of an incompressible Carreau fluid is investigated in eccentric cylinders. The problem is measured in cylindrical coordinates. The governing equations are observed under the conditions of long wavelength and low Reynolds number approximations. The resulting highly nonlinear second order partial differential equations are solved by series solution technique. The relation for pressure rise is evaluated numerically by built-in technique with the help of mathematics software. As a special case, the present results are compared with the existing results given in the literature. The obtained results are then plotted to see the influence of different physical parameters on the velocity, pressure gradient and pressure rise expressions. The velocity profile is drawn for both two and three dimensions. The trapping boluses are also discussed through streamlines.

© 2013 Production and hosting by Elsevier B.V. on behalf of Ain Shams University.

1. Introduction

In the history of fluid dynamics, the area of peristaltic transportation has obtained significant attraction because of its considerable contribution in the fields of engineering and biomechanics as this process remains vital in many biological mechanism and biomedical industry. Specifically, it is enormously applied in the pattern of swallowing food through the esophagus, chyme motion in the gastrointestinal tract, vasomotion of small blood vessels such as venules, capillaries and arterioles, urine transport flow from kidney to bladder, sanitary fluid transportation and transportation of corrosive fluids and a toxic liquid flow in the nuclear industry. In the view of such immense contribution of peristaltic flows in engineering and biomedical many researchers have focused on the study of peristaltic mechanism. Naturally, the behavior of frequently used fluids in such type of phenomena is mostly non-Newtonian to intensive extent. Keeping in mind the complexity of non-Newtonian fluids, many of the researchers have

* Corresponding author. Tel.: +92 3339822640/+92 3006076036.
E-mail address: ariiui@hotmail.com (A. Riaz).
Peer review under responsibility of Ain Shams University.

Production and hosting by Elsevier

2090-4479 © 2013 Production and hosting by Elsevier B.V. on behalf of Ain Shams University.
http://dx.doi.org/10.1016/j.asej.2013.09.005

worked on the peristaltic flows of different non-Newtonian models in the sense of constitutive relations. In the studies [1–11], the researchers have obtained the various results regarding peristaltic flows in different types of flow geometries. A lot of literature is available on the topic of analytical and numerical treatment of Newtonian and non-Newtonian fluids [12–14].

Hydromagnetic flow of fluid with variable viscosity in a uniform tube with peristalsis has been investigated by El Hakeem et al. [15]. Hariharan et al. [16] have presented the peristaltic transport of non-Newtonian fluid in a diverging tube with different wave forms. Few years ago, Ebaid [17] has analyzed a new numerical solution for the MHD peristaltic flow of a biofluid with variable viscosity in circular cylindrical tube via Adomian decomposition method. The influence of heat and mass transfer on MHD peristaltic flow through a porous space with compliant walls has been manipulated by Srinivas and Kothandapani [18]. Mekheimer [19] have shown the effect of the induced magnetic field on peristaltic flow of a couple stress fluid.

All the above mentioned problems have been discussed for two dimensional geometries. Nowadays, the researchers are going to concentrate on the three dimensional flows of different non-Newtonian models for the fluids having different physical behaviors. Subba Reddy et al. [20] have discussed the influence of lateral walls on peristaltic flow in a rectangular duct. They found the exact solutions for the flow problem and shown the effects of various physical parameters. A mathematical model for the flow of micropolar fluid through catheterized artery has been analyzed by Srinivasacharya and Srikanth [21]. These three dimensional studies are considered in Cartesian coordinate system. There are very rare cases which deal with the three dimensional cylindrical coordinates for peristaltic flow problem. Only a couple of articles [22,23] have been reported which incorporate the peristaltic transport in eccentric cylinders. However, the peristaltic flow of non-Newtonian Carreau fluid model is not measured yet in eccentric cylinders.

Keeping in mind the mechanical, physiological, and industrial applications of peristaltic flows of non-Newtonian fluids, the authors are motivated to work on the peristaltic flow of Carreau fluid flowing between two eccentric cylinders. The governing equations are modeled under the system of cylindrical coordinates. The problem is simplified after the implementation of long wavelength and low Reynolds number approximations. The analytical results are obtained by series solution technique. The expression for pressure rise is calculated numerically. The present results for velocity and pressure rise are also compared with that of the existing literature. The effects of all observing parameters on the profile of velocity, pressure gradient and pressure rise are shown graphically. The streamlines are also drawn for physical quantities occurred in the problem to observe the trapping bolus phenomenon.

2. Mathematical formulation of the problem

Let us observe the peristaltic flow of incompressible Carreau fluid flowing between the two eccentric cylinders. The flow geometry is arranged as the inner tube is rigid and sinusoidal

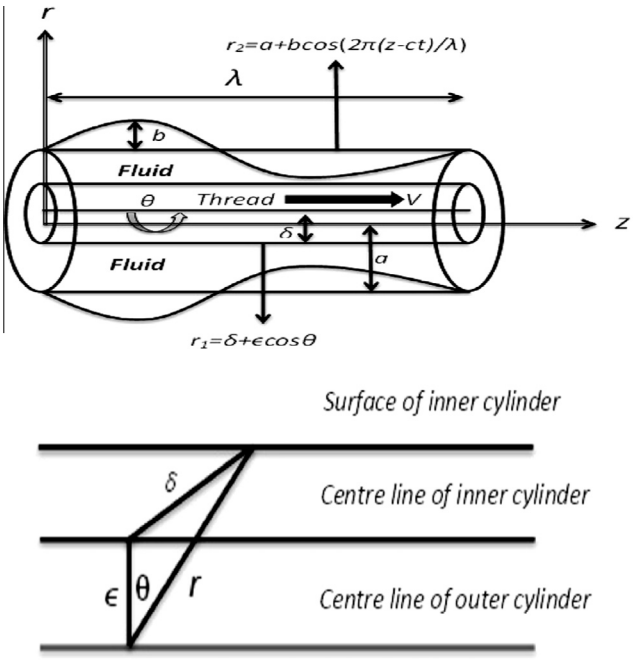

Figure 1 The simplified model of geometry of the problem.

wave is propagating at the outer tube along its length. The inner tube has radius δ but we consider the fluid motion to the center of the outer tube. The center of the inner tube is now at the position $r = \epsilon$, $z = 0$, where r and z are coordinates in the cross-section of the pipe as shown in Fig. 1. The boundary of the inner tube is measured to order ϵ by $r_1 = \delta + \epsilon\cos\theta$, where ϵ is the parameter that controls the eccentricity of the inner tube position.

The equations for the walls are described as [22]

$$r_1 = \delta + \epsilon\cos\theta,$$
$$r_2 = a + b\cos\left[\frac{2\pi}{\lambda}(z - ct)\right],$$

where δ and a are the radii of the inner and outer tubes, b is amplitude of the wave, λ is the wavelength, c is the propagation velocity and t is the time. The problem has been considered in the system of cylindrical coordinates (r, θ, z) as radial, azimuthal and axial coordinates, respectively.

The equations of mass and momentum for an incompressible Carreau fluid are described as

$$\text{div } \mathbf{V} = 0, \tag{1}$$
$$\rho\frac{d\mathbf{V}}{dt} = -\nabla p + \text{div}\boldsymbol{\tau}, \tag{2}$$

where ρ is the density, d/dt is the material time derivative, $\mathbf{V}$ is the velocity field, dp/dz is the pressure, τ is the constitutive relation for Carreau fluid. According to the nature of the flow, the velocity field is taken as $\mathbf{V} = (v, w, u)$. Using this velocity field, Eqs. (1) and (2) are respectively written as

Table 1 Comparison of velocity distribution of present work with Mekheimer et al. [22].

r	Mekheimer et al. [22]	Present work	
	$u(r,\theta,z,t)$	$u(r,\theta,z,t)$ for $We = 0$, $n = 0$	$u(r,\theta,z,t)$ for $We = 0.5$, $n = 2$
0.20	0.1000	0.1000	0.1000
0.25	0.1093	0.1096	0.1103
0.30	0.1119	0.1119	0.1142
0.35	0.1119	0.1114	0.1137
0.40	0.1096	0.1098	0.1100
0.45	0.1054	0.1056	0.1041
0.50	0.0995	0.0992	0.0964
0.55	0.0919	0.0916	0.0873
0.60	0.0829	0.0827	0.0771
0.65	0.0724	0.0726	0.0659
0.70	0.0606	0.0601	0.0539
0.75	0.0474	0.0478	0.0412
0.80	0.0329	0.0337	0.0280
0.85	0.0171	0.0177	0.0142
0.90	0.0000	0.0000	0.0000

Table 2 Residue error for velocity profile u.

n	δ	ϕ	θ	z	t	Q	We	Residue
2	0.1	0.17	50°	0	0.4	0.9	1.000	−0.246548
							1.043	−0.226122
							1.086	−0.204769
							1.129	−0.182481
							1.172	−0.159250
							1.215	−0.135066
							1.258	−0.109921
							1.301	−0.083805
							1.344	−0.056707
							1.387	−0.028618
							1.430	0.0004728

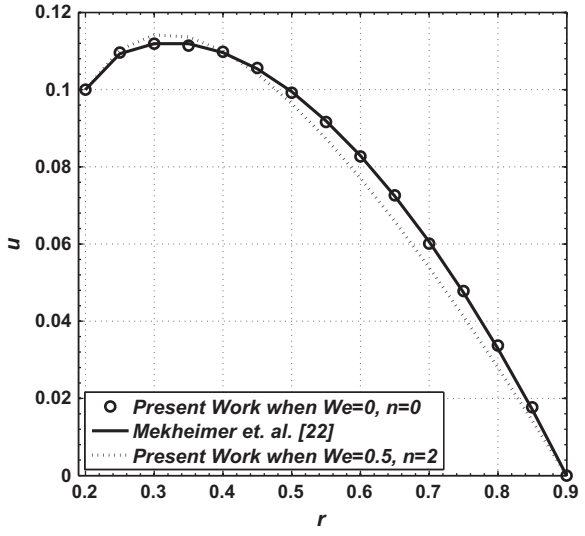

Figure 2 Comparison of velocity distribution of present work with [22] for fixed $\delta = 0.1$, $\theta = 0.01$, $\phi = 0.1$, $z = 0$, $t = 0.5$, $V = 0.1$, $\epsilon = 0.1$, and $Q = 0.69$.

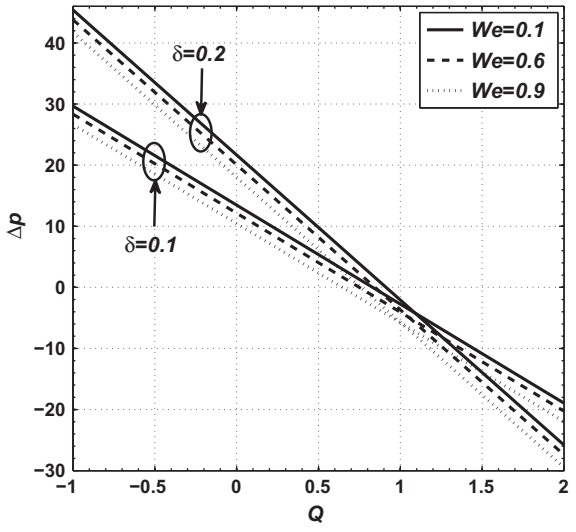

Figure 3 Variation in pressure rise Δp with δ and We for fixed $\epsilon = 0.1$, $\phi = 0.1$, $t = 0.1$, $\theta = 50^0$, $n = 2$, and $V = 0.9$.

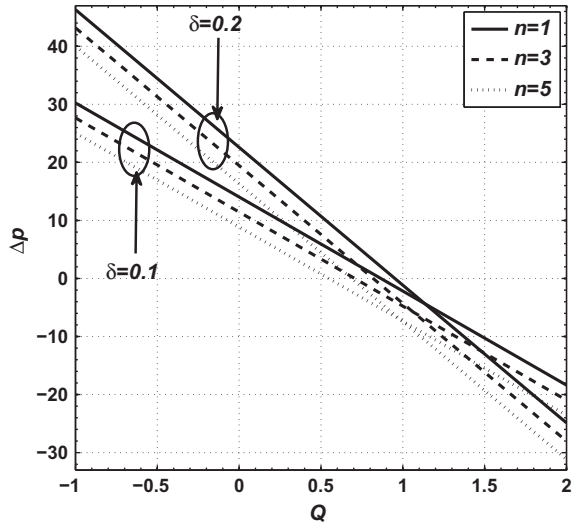

Figure 4 Variation in pressure rise Δp with δ and n for fixed $\epsilon = 0.1$, $We = 0.5$, $t = 0.1$, $\theta = 50^0$, $\phi = 0.2$, and $V = 1$.

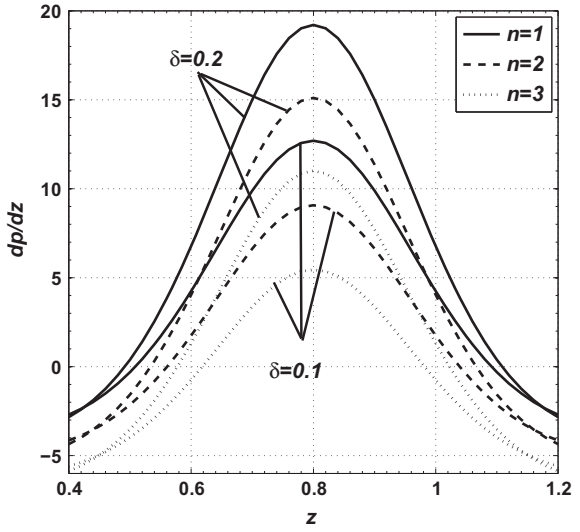

Figure 6 Variation in pressure gradient dp/dz with n and δ for fixed $\epsilon = 0.01$, $Q = 0.5$, $t = 0.3$, $\theta = 50^0$, $M = 0.5$, $\phi = 0.1$, and $V = 0.3$.

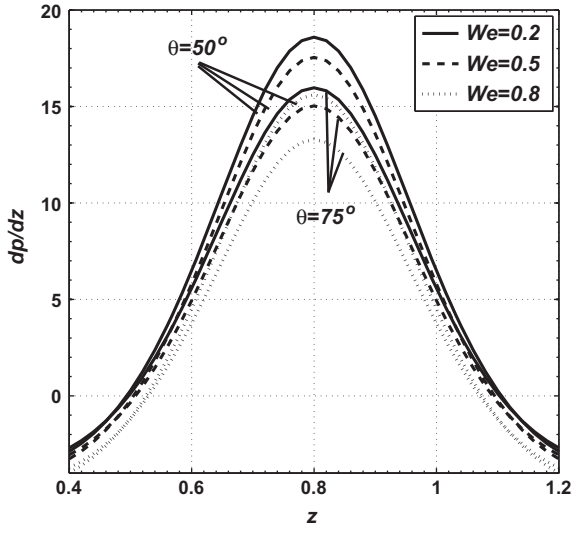

Figure 5 Variation in pressure gradient dp/dz with θ and We for fixed $\epsilon = 0.1$, $V = 0.9$, $t = 0.3$, $n = 2$, $\phi = 0.1$, $Q = 0.2$, and $\delta = 0.2$.

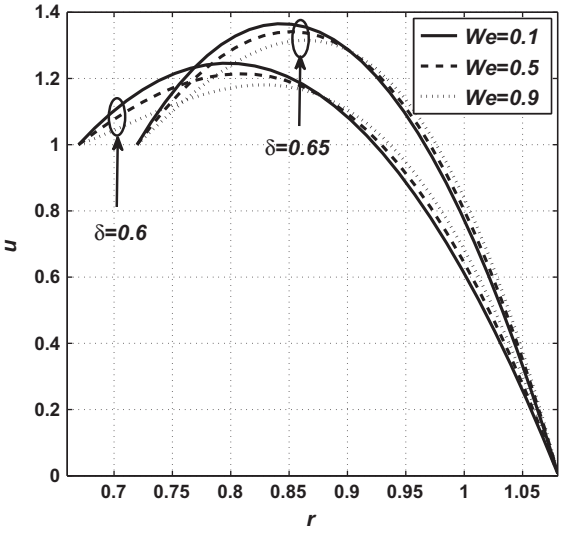

Figure 7 Variation in velocity profile u with δ and We for fixed $\epsilon = 0.1$, $Q = 0.5$, $t = 0.1$, $z = 0$, $V = 1$, $\theta = 50^0$, $\phi = 0.1$, and $n = 4$, (a) for 2-dimensional and (b) for 3-dimensional.

$$\frac{\partial u}{\partial z}+\frac{\partial v}{\partial r}+\frac{v}{r}+\frac{1}{r}\frac{\partial w}{\partial \theta}=0, \tag{3}$$

$$\rho\left[\frac{\partial v}{\partial t}+u\frac{\partial v}{\partial z}+v\frac{\partial v}{\partial r}+\frac{w}{r}\frac{\partial v}{\partial \theta}-\frac{w^2}{r}\right]=-\frac{\partial p}{\partial r}+\frac{1}{r}\frac{\partial}{\partial r}(r\tau_{rr})+\frac{1}{r}\frac{\partial}{\partial \theta}(\tau_{r\theta})+\frac{\partial}{\partial z}(\tau_{rz})-\frac{\tau_{\theta\theta}}{r}, \tag{4}$$

$$\rho\left[\frac{\partial w}{\partial t}+u\frac{\partial w}{\partial z}+v\frac{\partial w}{\partial r}+\frac{w}{r}\frac{\partial w}{\partial \theta}-\frac{wv}{r}\right]=-\frac{1}{r}\frac{\partial p}{\partial \theta}+\frac{1}{r^2}\frac{\partial}{\partial r}(r^2\tau_{r\theta})+\frac{1}{r}\frac{\partial}{\partial \theta}(\tau_{\theta\theta})+\frac{\partial}{\partial z}(\tau_{\theta z}), \tag{5}$$

$$\rho\left[\frac{\partial u}{\partial t}+u\frac{\partial u}{\partial z}+v\frac{\partial u}{\partial r}+\frac{w}{r}\frac{\partial u}{\partial \theta}\right]=-\frac{\partial p}{\partial z}+\frac{1}{r}\frac{\partial}{\partial r}(r\tau_{rz})+\frac{1}{r}\frac{\partial}{\partial \theta}(\tau_{\theta z})+\frac{\partial}{\partial z}(\tau_{zz}), \tag{6}$$

where , w and u are the velocity components in r, θ and z-directions, respectively, μ is the viscosity, τ_{rr}, $\tau_{r\theta}$, τ_{rz}, $\tau_{\theta\theta}$, $\tau_{\theta z}$ and τ_{zz} are stresses for Carreau fluid which can be manipulated with the expression of following stress [9]

$$\boldsymbol{\tau} = \mu(1+\Gamma^2\dot{\gamma}^2)^{\frac{(n-1)}{2}}\dot{\boldsymbol{\gamma}}.$$

In above relation, Γ and n are material coefficients. According to the present geometry, the boundary conditions are defined as

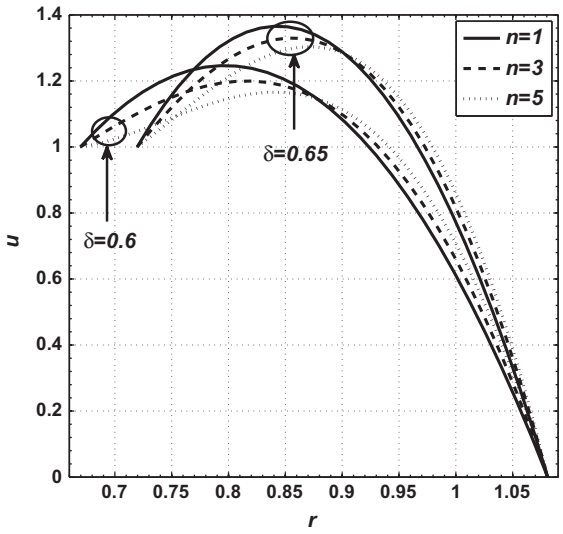

Figure 8 Variation in velocity profile u with δ and n for fixed $Q = 0.5$, $We = 1.5$, $t = 0.2$, $\epsilon = 0.1$, $z = 0.1$, $\theta = 50^0$, $\phi = 0.1$, and $V = 1$, (a) for 2-dimensional and (b) for 3-dimensional.

$$u = 0, \quad \text{at } r = r_2, \tag{7}$$
$$u = V, \quad \text{at } r = r_1, \tag{8}$$

where V stands for the velocity of inner tube. The velocity component in the azimuthal direction is assumed to be unaltered, so the velocity field is found as $(v, 0, u)$. The governing equations are non-dimensionalized by using the following dimensionless quantities

$$u' = \frac{u}{c},\ v' = \frac{\lambda}{ac}v,\ t' = \frac{c}{\lambda}t,\ r_1' = \frac{r_1}{a},\ \phi = \frac{b}{a},\ \delta' = \frac{\delta}{a},$$
$$\epsilon' = \frac{\epsilon}{a},\ \delta_0 = \frac{a}{\lambda},\ z' = \frac{z}{\lambda},$$
$$\dot{\gamma}' = \frac{a}{c}\dot{\gamma},\ r_2' = \frac{r_2}{a},\ \mathrm{Re} = \frac{\rho c a}{\mu},\ We = \frac{\Gamma c}{a},\ \tau' = \frac{a}{\mu c}\tau,$$
$$\theta' = \theta,\ p' = \frac{a^2}{\mu c \lambda}p,\ V' = \frac{V}{c},$$

where ϕ is the amplitude ratio, Re is the Reynolds number, δ_0 is the dimensionless wave number, ϵ is the eccentricity parameter, We is the Weissenberg number and τ is on stress coefficients. Making use of above dimensionless parameters, the governing equations (after neglecting primes) gain to the subsequent form

$$\frac{\partial v}{\partial r} + \frac{v}{r} + \frac{\partial u}{\partial z} = 0, \tag{9}$$
$$\mathrm{Re}\delta_0^3\left[\frac{\partial v}{\partial t} + u\frac{\partial v}{\partial z} + v\frac{\partial v}{\partial r}\right] = -\frac{\partial p}{\partial r} + \frac{\delta_0}{r}\frac{\partial}{\partial r}(r\tau_{rr}) + \frac{\delta_0}{r}\frac{\partial}{\partial \theta}(\tau_{r\theta}) + \delta_0^2\frac{\partial}{\partial z}(\tau_{rz}) - \delta_0\frac{\tau_{\theta\theta}}{r}, \tag{10}$$
$$0 = -\frac{1}{r}\frac{\partial p}{\partial \theta} + \frac{\delta_0}{r^2}\frac{\partial}{\partial r}(r^2\tau_{r\theta}) + \frac{\delta_0}{r}\frac{\partial}{\partial \theta}(\tau_{\theta\theta}) + \delta_0^2\frac{\partial}{\partial z}(\tau_{\theta z}), \tag{11}$$
$$\mathrm{Re}\delta_0\left[\frac{\partial u}{\partial t} + u\frac{\partial u}{\partial z} + v\frac{\partial u}{\partial r}\right] = -\frac{\partial p}{\partial z} + \frac{1}{r}\frac{\partial}{\partial r}(r\tau_{rz}) + \frac{1}{r}\frac{\partial}{\partial \theta}(\tau_{\theta z}) + \delta_0\frac{\partial}{\partial z}(\tau_{zz}). \tag{12}$$

The components of non-dimensional stresses for Carreau fluid are evaluated as

$$\tau_{rr} = 2\delta_0\left(1 + \frac{n-1}{2}We^2\dot{\gamma}^2\right)\frac{\partial v}{\partial r},$$
$$\tau_{r\theta} = \delta_0\left(1 + \frac{n-1}{2}We^2\dot{\gamma}^2\right)\frac{1}{r}\frac{\partial v}{\partial \theta},$$
$$\tau_{rz} = \left(1 + \frac{n-1}{2}We^2\dot{\gamma}^2\right)\left(\delta_0^2\frac{\partial v}{\partial z} + \frac{\partial u}{\partial r}\right),$$
$$\tau_{\theta\theta} = 2\delta_0\left(1 + \frac{n-1}{2}We^2\dot{\gamma}^2\right)\frac{v}{r},$$
$$\tau_{\theta z} = \left(1 + \frac{n-1}{2}We^2\dot{\gamma}^2\right)\frac{1}{r}\frac{\partial u}{\partial \theta},$$
$$\tau_{zz} = 2\delta_0\left(1 + \frac{n-1}{2}We^2\dot{\gamma}^2\right)\frac{\partial u}{\partial z},$$
$$\dot{\gamma}^2 = 2\delta_0^2\left(\frac{\partial v}{\partial r}\right)^2 + \frac{\delta_0^2}{r^2}\left(\frac{\partial v}{\partial \theta}\right)^2 + \left(\delta_0^2\frac{\partial v}{\partial z} + \frac{\partial u}{\partial r}\right)^2 + \frac{2\delta_0^2 v^2}{r^2} + \frac{1}{r^2}\left(\frac{\partial u}{\partial \theta}\right)^2 + 2\delta_0^2\left(\frac{\partial u}{\partial z}\right)^2. \tag{13}$$

Using the assumptions of long wavelength ($\delta_0 \to 0$) and low Reynolds number ($\mathrm{Re} \to 0$), the governing Eqs. (10)–(12) are simplified to the following form

$$\frac{\partial p}{\partial r} = 0, \tag{14}$$
$$\frac{\partial p}{\partial \theta} = 0, \tag{15}$$
$$\frac{\partial p}{\partial z} = \frac{\partial^2 u}{\partial r^2} + \frac{1}{r}\frac{\partial u}{\partial r} + \frac{1}{r^2}\frac{\partial^2 u}{\partial \theta^2} + \frac{n-1}{2}We^2\frac{\partial}{\partial r}\left(\frac{\partial u}{\partial r}\right)^3 + \frac{n-1}{2}We^2\frac{\partial}{\partial r}\left(\frac{1}{r^2}\frac{\partial u}{\partial r}\left(\frac{\partial u}{\partial \theta}\right)^2\right) + \frac{(n-1)We^2}{2r}\left(\left(\frac{\partial u}{\partial r}\right)^3 + \frac{1}{r^2}\frac{\partial u}{\partial r}\left(\frac{\partial u}{\partial \theta}\right)^2\right) + \frac{(n-1)We^2}{2r^2}\frac{\partial}{\partial \theta}\left(\frac{\partial u}{\partial \theta}\left(\frac{\partial u}{\partial r}\right)^2\right) + \frac{1}{r^2}\frac{\partial}{\partial \theta}\left(\frac{\partial u}{\partial \theta}\right)^3. \tag{16}$$

Eqs. (14) and (15) show that dp/dz is not a function of r and θ. The corresponding boundary conditions in non-dimensional form are

$$u = 0, \ \text{at } r = r_2 = 1 + \phi\cos[2\pi(z - t)], \tag{17}$$
$$u = V, \ \text{at } r = r_1 = \delta + \epsilon\cos\theta. \tag{18}$$

3. Solution of the problem

Solution of the above boundary value problem is obtained by series solution method [24]. The deformation equation for the given problem is defined as

$$H(u,f) = (1-f)(\mathcal{L}[\tilde{u}] - \mathcal{L}[\tilde{u}_0]) + f\left(\mathcal{L}[\tilde{u}] + \frac{1}{r}\frac{\partial u}{\partial r} + \frac{1}{r^2}\frac{\partial^2 u}{\partial \theta^2} + \frac{n-1}{2}We^2\frac{\partial}{\partial r}\left(\frac{\partial u}{\partial r}\right)^3 + \frac{n-1}{2}We^2\frac{\partial}{\partial r}\left(\frac{1}{r^2}\frac{\partial u}{\partial r}\left(\frac{\partial u}{\partial \theta}\right)^2\right) + \frac{(n-1)We^2}{2r}\left(\left(\frac{\partial u}{\partial r}\right)^3 + \frac{1}{r^2}\frac{\partial u}{\partial r}\left(\frac{\partial u}{\partial \theta}\right)^2\right) + \frac{(n-1)We^2}{2r^2}\left(\frac{\partial}{\partial \theta}\left(\frac{\partial u}{\partial \theta}\left(\frac{\partial u}{\partial r}\right)^2\right) + \frac{1}{r^2}\frac{\partial}{\partial \theta}\left(\frac{\partial u}{\partial \theta}\right)^3\right) - \frac{dp}{dz}\right) = 0, \tag{19}$$

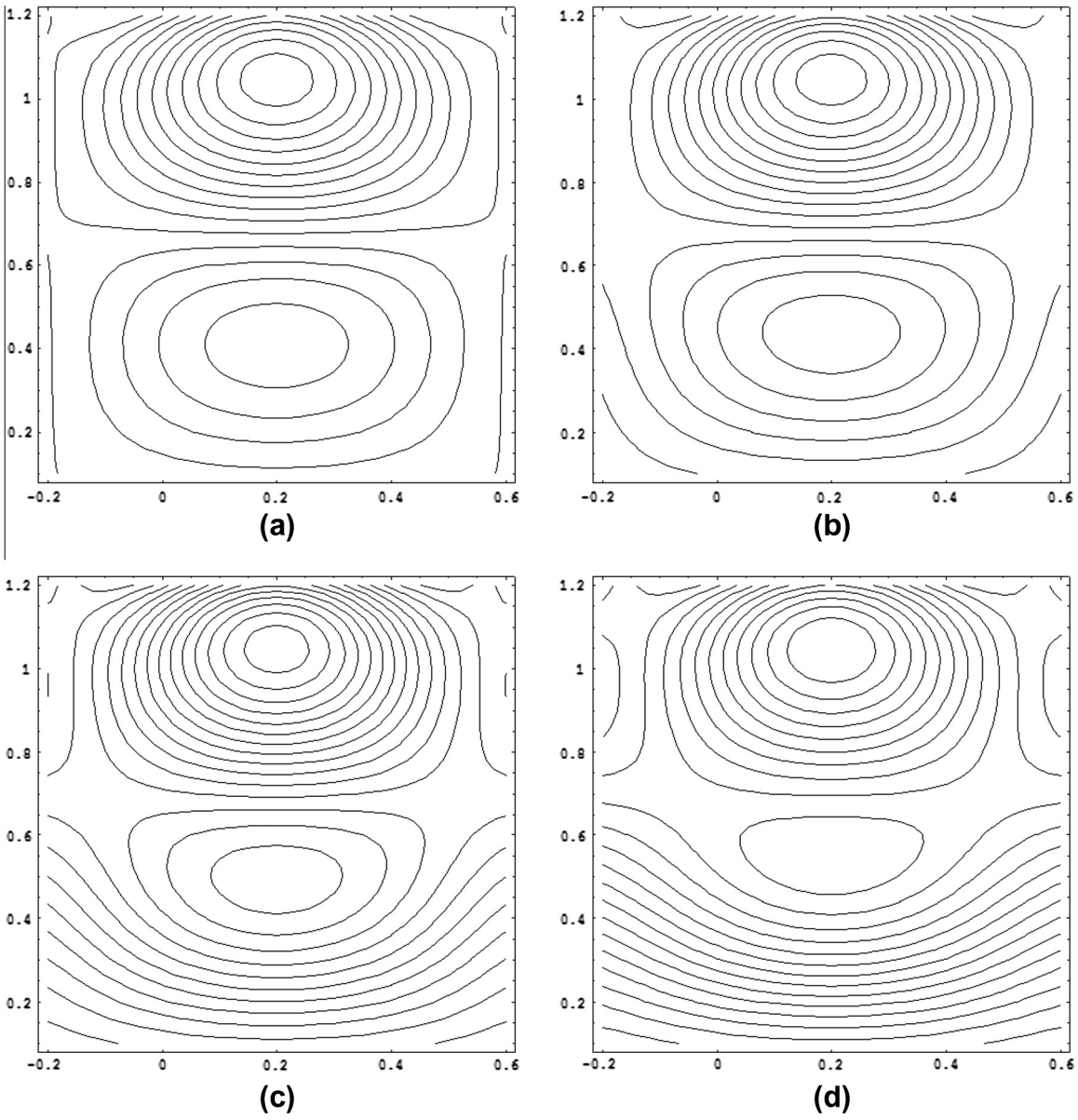

Figure 9 Stream lines for different values of We, (a) for $We = 0.1$, (b) for $We = 0.5$, (c) for $We = 0.9$, (d) for $We = 1.2$. The other parameters are $\epsilon = 0.3$, $Q = 0.2$, $V = 0.1$, $t = 0.2$, $\theta = 50^0$, $\phi = 0.05$, $\delta = 0.2$, and $n = 5$.

where $\mathcal{L}$, the linear operator is assumed to be $\mathcal{L} = \frac{\partial^2}{\partial r^2}$. We define the following initial guess satisfying the boundary conditions

$$\tilde{u}_0 = \frac{V(r - r_2)}{r_1 - r_2}. \tag{20}$$

Now we describe

$$\tilde{u}(r, \theta, z, t, q) = u_0 + f u_1 + f^2 u_2 + \ldots \tag{21}$$

Using the above equation into Eq. (19) and then finding the terms of first two orders of embedding parameter f, we get the following problems including boundary conditions

Zeroth order system

$$\mathcal{L}[u_0] - \mathcal{L}[\tilde{u}_0] = 0, \tag{22}$$

$$u_0 = 0, \quad \text{at } r = r_2, \tag{23}$$

$$u_0 = V, \quad \text{at } r = r_1. \tag{24}$$

The solution of the above zeroth order system can be obtained by using Eq. (20) and is simply found as

$$u_0(r, \theta, z, t, f) = \tilde{u}_o = \frac{V(r - r_2)}{r_1 - r_2}. \tag{25}$$

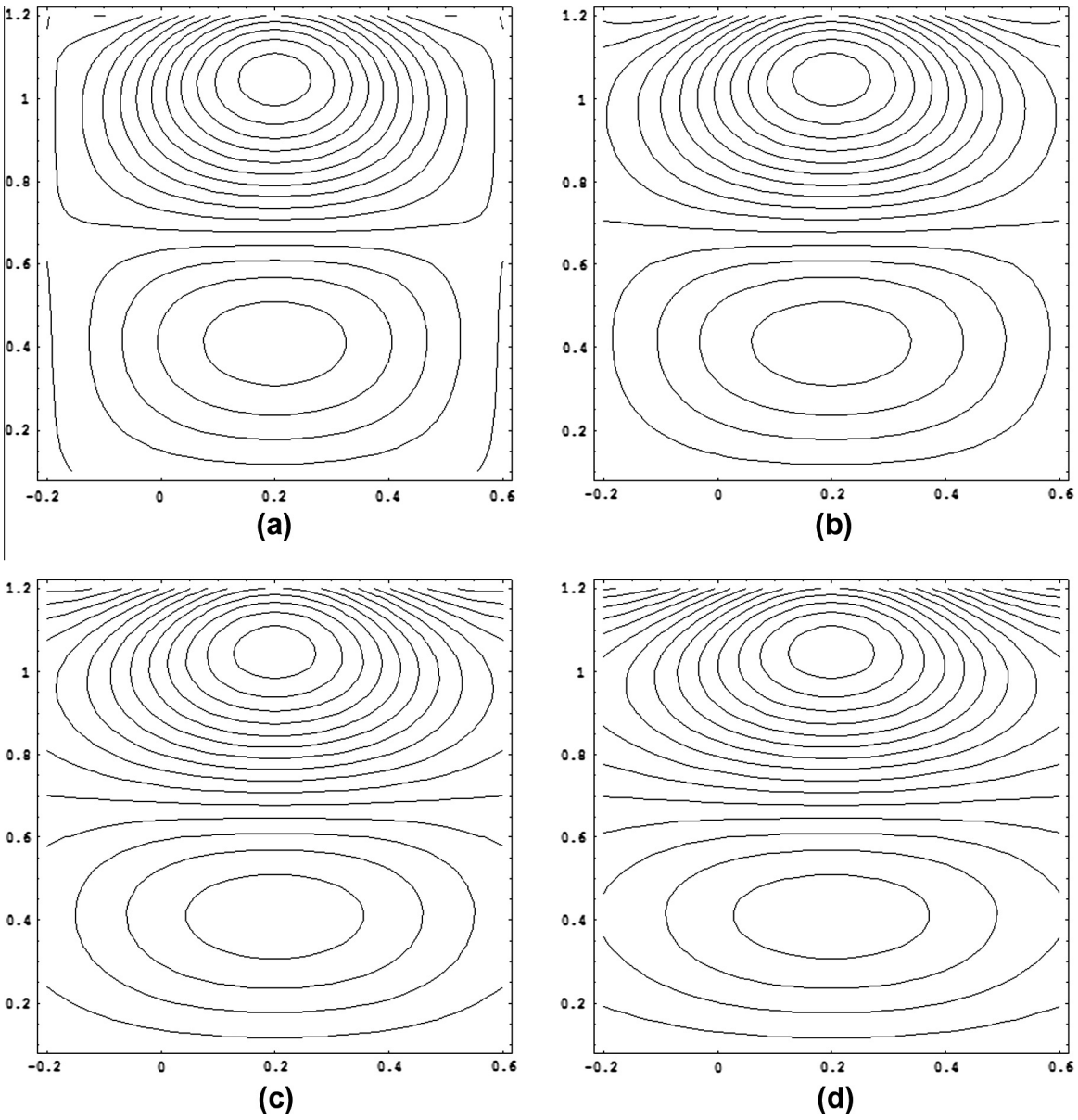

Figure 10 Stream lines for different values of Q, (a) for $Q = 0.2$, (b) for $Q = 0.3$, (c) for $Q = 0.4$, and (d) for $Q = 0.5$. The other parameters are $\epsilon = 0.3$, $t = 0.2$, $\theta = 50^0$, $V = 0.2$, $We = 0.3$, $n = 2$, $\delta = 0.2$, and $\phi = 0.05$.

First order system

$$\frac{\partial^2 u_1}{\partial r^2}+\frac{1}{r}\frac{\partial u_0}{\partial r}+\frac{1}{r^2}\frac{\partial^2 u_0}{\partial \theta^2}+\frac{n-1}{2}We^2\frac{\partial}{\partial r}\left(\frac{\partial u_0}{\partial r}\right)^3 + \frac{n-1}{2}We^2\frac{\partial}{\partial r}\left(\frac{1}{r^2}\frac{\partial u_0}{\partial r}\left(\frac{\partial u_0}{\partial \theta}\right)^2\right) + \frac{(n-1)We^2}{2r}\left(\left(\frac{\partial u_0}{\partial r}\right)^3+\frac{1}{r^2}\frac{\partial u_0}{\partial r}\left(\frac{\partial u_0}{\partial \theta}\right)^2\right) + \frac{(n-1)We^2}{2r^2}\left(\frac{\partial}{\partial \theta}\left(\frac{\partial u_0}{\partial \theta}\left(\frac{\partial u_0}{\partial r}\right)^2\right)+\frac{1}{r^2}\frac{\partial}{\partial \theta}\left(\frac{\partial u_0}{\partial \theta}\right)^3\right)-\frac{dp}{dz}=0, \quad (26)$$

$$u_1 = 0, \quad \text{at } r = r_2, \quad (27)$$

$$u_1 = 0, \quad \text{at } r = r_1. \quad (28)$$

The solution of the above linear ordinary differential equation is given in appendix. Finally, for $f \to 1$, we approach the final solution. So from Eq. (21), we get

$$u(r,\theta,z,t) = u_0 + u_1, \quad (29)$$

where u_0 and u_1 are defined in Eq. (25) and appendix, respectively. The instantaneous volume flow rate $Q(z,t)$ is given by

$$Q(z,t) = 2\pi\int_{r_1}^{r_2} rudr, \quad (30)$$

The mean volume flow rate $\overline{Q}$ over one period is given as [22]

$$\overline{Q}(z,t) = \frac{Q}{\pi} - \frac{\phi^2}{2} + 2\phi\cos[2\pi(z-t)] + \phi^2\cos^2[2\pi(z-t)], \quad (31)$$

Now pressure gradient dp/dz will be evaluated by using Eqs. (30) and (31) and is defined in appendix. The pressure rise $\Delta p(t)$ in non-dimensional form is defined as

$$\Delta p(t) = \int_0^1 \frac{\partial p}{\partial z} dz. \quad (32)$$

4. Results and discussion

In this section, we have discussed the effects of all the pertinent parameters on pressure rise, pressure gradient, velocity profile and streamlines with the help of graphs. As a special case of this problem, the comparison of the present work with that of Mekheimer et al. [22] is also manipulated through table and graph as well. The residue error is also presented to see the solution validity by varying certain quantities.

Table 1 shows the comparison of velocity variation in this article with the values obtained in [22]. In Table 2, the residue error analysis for velocity by varying different parameters is observed. Fig. 2 contains the graphs showing the velocity profile variation with emerging parameters for the present analysis and the old one. Figs. 3 and 4 tell us the variation in pressure rise Δp with the flow rate Q. We can observe the behavior of pressure gradient dp/dz with space coordinate z from Figs. 5 and 6. The graphs for the velocity profile u are displayed in Figs. 7 and 8. From Figs. 9 and 10, the trapping bolus phenomenon is discussed through streamlines for different effective parameters.

If we look at the Table 1, we can easily conclude that when we omit the effects of Carreau fluid parameters ($We = n = 0$), the present results are very much similar to that of given in Ref. [22]. From Fig. 2, it is clear that the present results for neglecting the effects of Carreau fluid overlaps the already produced results. It is also observed from Table 1 and Fig. 2 that when we include the Carreau fluid parameters ($We = 0.5$, $n = 2$), the velocity profile increases in the region $0.2 \leqslant r \leqslant 0.4$ but in the rest of the domain velocity decreases.

Fig. 3 has the variation in pressure rise Δp with δ and We. From this figure, it is measured that pressure rise Δp is varying directly with the increase in the values of δ in the retrograde pumping region ($\Delta p > 0, Q < 0$) and peristaltic pumping region ($\Delta p > 0, Q > 0$) but different observations are made for the augmented pumping region ($\Delta p < 0, Q > 0$). It is also revealed from this figure that pressure rise is reduced with the increase in We. It is observed from Fig. 4 that peristaltic pressure rise Δp is varying directly with the rising the magnitude of radius δ in retrograde pumping region and peristaltic pumping but reducing when observed in the augmented pumping region but decreasing with the power law index n.

Fig. 5 shows the effects of $\theta$and We on the expression of pressure gradient dp/dz. It is noted here that dp/dz is decreasing with the increase in We and θ. Fig. 6 is drawn to see the effect of $\delta$and n on the pressure gradient dp/dz against the coordinate z. We can say that pressure gradient gets inverse attitude when someone increases the magnitude of n but reverse behavior is reported when δ gets larger.

The velocity profile u with δ and We is sketched in Fig. 7 both for two and three dimensions. It is noted from this figure that u gets lessened with the increase in We in the part $0.6 \leqslant r \leqslant 0.9$ but in the remaining part u rises with We but in the whole region, velocity enlarges when δ gains larger values. When we look at Fig. 8, we can describe that it gives the similar behavior with the parameter δ and n as that of observed for δ and We in Fig. 7.

Fig. 9 gives the streamlines for the parameter We. t is noted from this figure that increasing the magnitude of We results in decreasing the number of bolus in both the parts of the geometry but size of the bolus is enlarged. Fig. 10 shows that the number of bolus is decreased but volume of the bolus expands when someone increases the numerical values of flow rate Q.

5. Concluding remarks

In the present investigation, analytical series solutions are presented for the peristaltic flow of Carreau fluid in gap between two eccentric tubes. The problem is measured under the assumptions of long wave length and low Reynolds number. The comparison of present analysis is also made with the existing literature. The main findings of the above work are as listed below

1. It is measured that in peristaltic pumping, the pressure rise curves rise up with δ but fall down with We and n.
2. It is observed that pressure rise is a decreasing function of We, n and θ while increasing function of radius δ .
3. From graphical results, we have seen that velocity profile is decreasing with the increase in We and n in left half of the domain but reverse attitude is measured in the right half while it increases with δ throughout the region.
4. It is depicted that number of bolus is changing inversely with We and Q but dimensions of the bolus increase.
5. It is also concluded that if we put $We = n = 0$ in the present analysis we get the results of previous work done by Mekheimer et al. [22].

Appendix A

$$
\begin{aligned}
u_1 = {} & \tfrac{1}{384r^2r_1^2(r_1-r_2)(r_2-\delta-\epsilon\cos\theta)^7}\Big(288r^2r_1^2(r-r_2)(r_1-r_2)V(r_2-\delta)\epsilon(8(r_2-\delta)^4+20(r_2-\delta)^2\epsilon^2+5\epsilon^4)\cos\theta\\
& -3\tfrac{dp}{dz}r^2(r-r_1)r_1^2(r-r_2)(r_1-r_2)\epsilon^7\cos 7\theta+3r^2r_1^2(r-r_2)\times(-r_1+r_2)\epsilon^5\cos 5\theta(48V(-r_2+\delta)\\
& +7\tfrac{dp}{dz}(r-r_1)(12(r_2-\delta)^2+\epsilon^2)+24V(r_2-\delta)(\log(r)-\log(r_1)))+6r^2r_1^2\epsilon^6\cos 6\theta((r-r_2)(r_1-r_2)\big(-2V+7\tfrac{dp}{dz}(r-r_1)(r_2-\delta)\big)\\
& +2r_2V((-r_1+r_2)\log(r)+(r-r_2)\log(r_1)+(-r+r_1)\log(r_2)))+4\epsilon^4\cos 4\theta\big((r-r_2)(r_1-r_2)\big(21\tfrac{dp}{dz}r^2\times(r-r_1)r_1^2(r_2-\delta)\\
& \times(10(r_2-\delta)^2+3\epsilon^2)+V\big((-1+n)r_1^2r_2(1+3r_2)V^2We^2-5(-1+n)\times r_1(1+6r_2)V^2We^2+18\\
& \times r_1^2(10(r_2-\delta)^2+\epsilon^2)\big)\big)\big)+6r^2r_1^2V((r_1-r_2)(26r(r_2-\delta)^2+4r\epsilon^2+r_2(8(-1+n)V^2We^2-4\\
& \times(r_2-\delta)^2+\epsilon^2))\log(r)-(r-r_2)(26r_1(r_2-\delta)^2+4r\times\epsilon^2+r_2(8(-1+n)V^2We^2-4(r_2-\delta)^2\\
& +\epsilon^2))\log(r_1)+(r-r_1)r_2(8(-1+n)V^2We^2+22(r_2-\delta)^2+5\epsilon^2)\log(r_2))\big)+2\epsilon^2\cos 2\theta\\
& \times((r-r_2)(r_1-r_2)\big(21\tfrac{dp}{dz}r^2(r-r_1)r_1^2(r_2-\delta)\times(48(r_2-\delta)^4+80(r_2-\delta)^2\epsilon^2+15\epsilon^4)+2V\\
& \times(-4(-1+n)rr_1^2V^2We^2((5+6r_2)(r_2-\delta)^2-48r_2\epsilon^2)+4(-1+n)r_1^2r_2V^2We^2((r_2-\delta)^2-6r_2\epsilon^2)\\
& -r^2(4(-1+n)r_2V^2We^2((r_2-\delta)^2-6r_2\epsilon^2)+4(-1+n)r_1V^2We^2(-(5+6r_2)(r_2-\delta)^2+48r_2\epsilon^2)\\
& +45r_1^2(16(r_2-\delta)^4+16(r_2-\delta)^2\epsilon^2+\epsilon^4)))\big)-6r^2r_1^2V(-(r_1-r_2)(8(-5(-1+n)V^2We^2\\
& +r_2((-1+n)V^2\times We^2+6(r_2-\delta)^2))(r_2-\delta)^2+8(-(-1+n)V^2We^2+r_2(-17(-1+n)V^2We^2\\
& +20\times(r_2-\delta)^2))\epsilon^2+17r_2\epsilon^4+8r((-(-1+n)V^2We^2+36(r_2-\delta)^2)(r_2-\delta)^2+5(-(-1+n)\\
& \times V^2We^2+10(r_2-\delta)^2)\epsilon^2+4\epsilon^4))\log(r)+(r-r_2)(8(-5(-1+n)V^2We^2+r_2((-1+n)\times We^2\\
& +6(r_2-\delta)^2))(r_2-\delta)^2+8(-(-1+n)V^2We^2+r_2(-17(-1+n)V^2We^2+20(r_2-\delta)^2))\epsilon^2+17r_2\epsilon^4\\
& +8r_1((-(-1+n)V^2We^2+36(r_2-\delta)^2)(r_2-\delta)^2+5(-(-1+n)\times V^2We^2+10(r_2-\delta)^2)\epsilon^2+4\epsilon^4))\log(r_1)\\
& +(r-r_1)(-8(-5(-1+n)V^2We^2+42r_2\times(r_2-\delta)^2)(r_2-\delta)^2-8(-(-1+n)\times\\
& V^2We^2+2r_2(-11(-1+n)V^2We^2+35(r_2-\delta)^2))\epsilon^2-49r_2\epsilon^4)\log(r_2)))+\epsilon\cos\theta(-(r-r_1)\times\\
& \times(r-r_2)(r_1-r_2)(8(-1+n)\big(-10rr_1+2(r+r_1+6rr_1)r_2-3(r+r_1)r_2^2\big)V^3We^2(r_2-\delta)\epsilon^2+21\tfrac{dp}{dz}r^2r_1^2(64(r_2-\delta)^6+240(r_2-\delta)^4\epsilon^2\\
& +120(r_2-\delta)^2\epsilon^4+5\epsilon^6))-48r^2r_1^2V(r_2-\delta)\times((r_1-r_2)(4(-4(-1+n)\times V^2We^2+r_2((-1+n)V^2We^2+2(r_2-\delta)^2))(r_2-\delta)^2\\
& +2\times(-7(-1+n)V^2We^2+r_2(11(-1+n)V^2We^2+38(r_2-\delta)^2))\epsilon^2+33r_2\epsilon^4+r(4((-1+n)\\
& V^2We^2+14\times(r_2-\delta)^2)(r_2-\delta)^2+4(5(-1+n)V^2We^2+49(r_2-\delta)^2)\epsilon^2+63\epsilon^4))\times \qquad \log r+(-r+r_2)(4(-4(-1+n)V^2We^2\\
& +r_2((-1+n)V^2We^2+2(r_2-\delta)^2))(r_2-\delta)^2+2(-7(-1+n)V^2We^2+r_2(11(-1+n)V^2We^2+38(r_2-\delta)^2))\epsilon^2+33r_2\epsilon^4+r_1\\
& \times(4((-1+n)V^2We^2+14(r_2-\delta)^2)(r_2-\delta)^2+4(5(-1+n)V^2We^2+49(r_2-\delta)^2)\epsilon^2+63\epsilon^4))\log(r_1)+2(r-r_1)(4(-2(-1+n)V^2We^2\\
& +r_2((-1+n)V^2We^2+8\times(r_2-\delta)^2))(r_2-\delta)^2+(-7(-1+n)V^2We^2+r_2(21(-1+n)V^2We^2+136\times(r_2-\delta)^2))\epsilon^2+48r_2\epsilon^4)\log(r_2)))\\
& +4((r-r_2)(r_1-r_2)\big(3\tfrac{dp}{dz}r^2(r-r_1)r_1^2\times(r_2-\delta)(16(r_2-\delta)^6+168(r_2-\delta)^4\epsilon^2+210(r_2-\delta)^2\epsilon^4+35\epsilon^6)\\
& +V\times((-1+n)r_1^2r_2V^2We^2\epsilon^2(-4(r_2-\delta)^2+(-1+21r_2)\epsilon^2)+r^2\times((-1+n)r_2V^2\times We^2\epsilon^2(-4(5+6r_2)(r_2-\delta)^2\\
& +(-5+162r_2)\epsilon^2)6r_1^2(-16(r_2-\delta)^6-120(r_2-\delta)^4\epsilon^2-90(r_2-\delta)^2\epsilon^4-5\epsilon^6))\big)\\
& +6r^2r_1^2V((r_1-r_2)(8(-(-1+n)\times V^2We^2+2\times r(r_2-\delta)^2)(r_2-\delta)^4+4(-7(-1+n)V^2We^2+r_2(5(-1+n)V^2We^2\\
& +14(r_2-\delta)^2)+r\times(7(-1+n)V^2We^2+44(r_2-\delta)^2))(r_2-\delta)^2\epsilon^2+2(-2\times(-1+n)V^2We^2\\
& +2r_2(17(-1+n)V^2We^2+21(r_2-\delta)^2)+r(14(-1+n)V^2\times We^2+87(r_2-\delta)^2))\epsilon^4\\
& +(12r+7r_2)\epsilon^6)\log(r)+(-r+r_2)(8(-(-1+n)V^2\times We^2+2r_1(r_2-\delta)^2)(r_2-\delta)^4+4(-7(-1+n)V^2We^2\\
& +r_2\times(5(-1+n)V^2We^2+14(r_2-\delta)^2)+r_1(7(-1+n)V^2We^2+44(r_2-\delta)^2))(r_2-\delta)^2\epsilon^2\\
& +2\times(-2\times(-1+n)V^2We^2+2r_2(17(-1+n)V^2We^2+21(r_2-\delta)^2)+r_1(14(-1+n)V^2\times We^2\\
& +87(r_2-\delta)^2))\epsilon^4+(12r_1+7r_2)\epsilon^6)\log(r_1)+(r-r_1)(8(-(-1+n)V^2\times We^2+2r_2(r_2-\delta)^2)\\
& \times(r_2-\delta)^4+4(-7(-1+n)V^2We^2+2r_2(6(-1+n)V^2We^2+29(r_2-\delta)^2))(r_2-\delta)^2\epsilon^2+2\\
& \times(-2(-1+n)V^2We^2+3r_2(16(-1+n)V^2We^2+43(r_2-\delta)^2))\epsilon^4+19r_2\epsilon^6)\log(r_2)))+\epsilon^3\\
& \times\cos 3\theta\Big((r-r_2)(-r_1+r_2)\Big(21\tfrac{dp}{dz}r^2(r-r_1)r_1^2(80(r_2-\delta)^4+60(r_2-\delta)^2\epsilon^2+3\epsilon^4)-8V\\
& \times(r_2-\delta)((-1+n)r_1^2\times r_2(-2+3r_2)V^2We^2-2(-1+n)rr_1^2(-5+6r_2)V^2We^2\\
& +r^2(-(-1+n)r_2(-2+3r_2)V^2We^2+2(-1+n)r_1(-5+6r_2)V^2We^2+30r_1^2(8(r_2-\delta)^2+3\epsilon^2)))\Big)\\
& +24r^2r_1^2\times V(r_2-\delta)((-r_1+r_2)(-4(-1+n)V^2We^2+r_2(-20(-1+n)V^2We^2+8(r_2-\delta)^2+17\epsilon^2)\\
& +r\times(-16(-1+n)V^2We^2+88(r_2-\delta)^2+47\epsilon^2))\log(r)+(r-r_2)(-4(-1+n)V^2We^2\\
& +r_2(-20\times(-1+n)V^2We^2+8(r_2-\delta)^2+17\epsilon^2)+r_1(-16(-1+n)V^2We^2+88(r_2-\delta)^2+47\epsilon^2))\\
& \times\log(r_1)-4(r-r_1)(-(-1+n)V^2We^2+r_2(-9(-1+n)V^2We^2+24(r_2-\delta)^2+16\epsilon^2))\times\log(r_2)))).
\end{aligned}
$$

$$\frac{dp}{dz}=\frac{1}{48\pi r_1^2(r_1-r_2)^3(r_1+r_2)(r_2-\delta-\epsilon\cos\theta)^7}\Big(2(36Qr_1^2(r_2-\delta)(16(r_2-\delta)^6$$
$$+168(r_2-\delta)^4\epsilon^2+210(r_2-\delta)^2\epsilon^4+35\epsilon^6)-\pi(r_1-r_2)V((-1+n)r_2^3V^2We^2\epsilon^2(4(r_2-\delta)^2+(1-21r_2)\epsilon^2)$$
$$+(-1+n)r_1r_2^2V^2We^2\epsilon^2(-8(2+3r_2)(r_2-\delta)^2+(-4+141r_2)\epsilon^2)$$
$$+4r_1^4(64(r_2-\delta)^6+4(7(-1+n)V^2We^2+134(r_2-\delta)^2)(r_2-\delta)^2\epsilon^2+4(7(-1+n)$$
$$V^2We^2+111(r_2-\delta)^2)\epsilon^4+27\epsilon^6)+r_1^2r_2(-8(9(-1+n)V^2We^2+4r_2(r_2-\delta)^2)(r_2-\delta)^4$$
$$+4(-49(-1+n)V^2We^2+r_2(85(-1+n)V^2We^2+122(r_2-\delta)^2))(r_2-\delta)^2\epsilon^2+2(-11$$
$$(-1+n)V^2We^2+2r_2(79(-1+n)V^2We^2+228(r_2-\delta)^2))\epsilon^4+81r_2\epsilon^6)+r_1^3(-8(9(-1+n)V^2We^2$$
$$+4r_2(r_2-\delta)^2)(r_2-\delta)^4+4(-68(-1+n)V^2We^2+r_2(67(-1+n)V^2We^2$$
$$+122(r_2-\delta)^2))(r_2-\delta)^2\epsilon^2+(-41(-1+n)V^2We^2+2r_2(443(-1+n)V^2We^2+456(r_2-\delta)^2))\epsilon^4+81r_2\epsilon^6)))$$
$$+2304\pi r_1^2\phi\cos2\pi(z-t)(r_2-\delta-\epsilon\cos\theta)^7-9r_1^2\epsilon^7(2Q+\pi\phi^2$$
$$\cos4\pi(z-t))\cos7\theta+3r_1^2\epsilon^5\cos5\theta(2(\pi(28r_1^3-45r_1^2r_2+17r_2^3)V-252Q(r_2-\delta))$$
$$(r_2-\delta)-42Q\epsilon^2+3\pi(-7(12(r_2-\delta)^2+\epsilon^2)\phi^2\cos4\pi(z-t)+4r_2^3V\times(r_2-\delta)$$
$$(\log(r_1)-\log(r_2))))+\epsilon\cos\theta(2(63Qr_1^2(-64(r_2-\delta)^6-240(r_2-\delta)^4\epsilon^2-120(r_2-\delta)^2$$
$$\epsilon^4-5\epsilon^6)+2\pi(r_1-r_2)V(r_2-\delta)(-(-1+n)r_2^3(-2+3r_2)V^2We^2\epsilon^2+(-1+n)r_1r_2^2$$
$$(-8+9r_2)V^2We^2\epsilon^2+4r_1^4(4((-1+n)V^2We^2+50(r_2-\delta)^2)(r_2-\delta)^2+4(5(-1+n)$$
$$V^2We^2+139(r_2-\delta)^2)\epsilon^2+153\epsilon^4)+r_1^2r_2(4(-36(-1+n)V^2We^2+r_2(13\times(-1+n)$$
$$V^2We^22(r_2-\delta)^2))(r_2-\delta)^2+2(-49(-1+n)V^2We^2+11r_2(11(-1+n)V^2We^2+34$$
$$(r_2-\delta)^2))\epsilon^2+369r_2\epsilon^4)+r_1^3(4(-36(-1+n)V^2We^2+r_2(13(-1+n)V^2We^2$$
$$2(r_2-\delta)^2))(r_2-\delta)^2+2(-68(-1+n)V^2We^2+r_2(145(-1+n)V^2We^2+374(r_2-\delta)^2))\epsilon^2+369r_2\epsilon^4)))$$
$$+3\pi r_1^2(-21(64(r_2-\delta)^6+240(r_2-\delta)^4\epsilon^2+120(r_2-\delta)^2$$
$$\epsilon^4+5\epsilon^6)\phi^2\cos4\pi(z-t)-8V(r_2-\delta)(r_2^2(4(-4(-1+n)V^2We^2+r_2((-1+n)V^2$$
$$We^2+2(r_2-\delta)^2))(r_2-\delta)^2+(-12(-1+n)V^2We^2+19r_2((-1+n)V^2We^2+4(r_2-\delta)^2))\epsilon^2+33r_2\epsilon^4)$$
$$+2r_1^2(4(-2(-1+n)V^2We^2+r_2((-1+n)V^2We^2+8(r_2-\delta)^2))$$
$$(r_2-\delta)^2+(-7(-1+n)V^2We^2+r_2(21(-1+n)V^2We^2+136(r_2-\delta)^2))\epsilon^2+48r_2\epsilon^4)$$
$$2r_1r_2(4(-2(-1+n)V^2We^2+r_2((-1+n)V^2We^2+8(r_2-\delta)^2))(r_2-\delta)^2+(-7(-1+n)V^2We^2+r_2(21(-1+n)V^2We^2$$
$$+136(r_2-\delta)^2))\epsilon^2+48r_2\epsilon^4))(\log(r_1)-\log(r_2))))$$
$$+\epsilon^2\cos2\theta\Big(252Qr_1^2(r_2-\delta)(48(r_2-\delta)^4+80(r_2-\delta)^2\epsilon^2+15\epsilon^4)-\pi(r_1-r_2)V\times$$
$$(16(-1+n)r_1r_2^2V^2We^2((2+3r_2)(r_2-\delta)^2-21r_2\epsilon^2)+8(-1+n)r_2^3V^2We^2(-(r_2-\delta)^2+6r_2\epsilon^2)$$
$$+4r_1^4(8(-(-1+n)V^2We^2+126(r_2-\delta)^2)(r_2-\delta)^2+40(-(-1+n)V^2We^2$$
$$+28(r_2-\delta)^2)\epsilon^2+77\epsilon^4)+r_1^3(8(-40(-1+n)V^2We^2+r_2(11(-1+n)V^2We^2+18(r_2-\delta)^2))(r_2-\delta)^2$$
$$+8(-9(-1+n)V^2We^2+r_2(-221(-1+n)V^2We^2+200(r_2-\delta)^2))\epsilon^2+191r_2\epsilon^4)+r_1^2r_2(8(-59(-1+n)V^2We^2+$$
$$r_2(-7(-1+n)V^2We^2+18(r_2-\delta)^2))(r_2-\delta)^2+8(-9(-1+n)V^2We^2+r_2(-53(-1+n)V^2We^2+200(r_2-\delta)^2))\epsilon^2+191r_2\epsilon^4))+$$
$$6\pi r_1^2(21(r_2-\delta)(48(r_2-\delta)^4+80(r_2-\delta)^2\epsilon^2+15\epsilon^4)\phi^2\cos4\pi(z-t)+V(r_2^2(8\times(-6(-1+n)V^2We^2$$
$$+r_2((-1+n)V^2We^2+6(r_2-\delta)^2))(r_2-\delta)^2+8(-(-1+n)V^2We^2+r_2(-11(-1+n)V^2We^2+20(r_2-\delta)^2))\epsilon^2+17r_2\epsilon^4)$$
$$+r_1^2(8(-5(-1+n)V^2We^2+42r_2(r_2-\delta)^2)(r_2-\delta)^2+8(-(-1+n)V^2We^2+2r_2(-11(-1+n)V^2We^2+35(r_2-\delta)^2))\epsilon^2$$
$$+49r_2\epsilon^4)+r_1r_2(8(-5(-1+n)V^2We^2+42r_2(r_2-\delta)^2)(r_2-\delta)^2+8(-(-1+n)V^2We^2$$
$$+2r_2(-11(-1+n)V^2We^2+35(r_2-\delta)^2))\epsilon^2+49r_2\epsilon^4))(\log(r_1)-\log(r_2)))\Big)$$
$$+2\epsilon^4\cos4\theta\Big(252Qr_1^2(r_2-\delta)(10(r_2-\delta)^2+3\epsilon^2)-\pi(r_1-r_2)V(-(-1+n)r_2^3(1+3r_2)V^2We^2+$$

$$+(-1+n)r_1r_2^2(4+27r_2)V^2We^2+4r_1^4(116(r_2-\delta)^2+13\epsilon^2)+r_1^3(5(-1+n)V^2We^2-2r_2(-51(-1+n)V^2We^2+56(r_2-\delta)^2)+7r_2\epsilon^2)$$
$$+7r_1^2r_2(-2(-1+n)V^2We^2+r_2(-16(r_2-\delta)^2+\epsilon^2)))+6\pi r_1^2(21(r_2-\delta)(10(r_2-\delta)^2+3\epsilon^2)\phi^2\cos 4\pi(z-t)+r_2V(r_1^2(8(-1$$
$$+n)V^2We^2+22(r_2-\delta)^2+5\epsilon^2)+r_1r_2(8(-1+n)V^2We^2+22(r_2-\delta)^2$$
$$+5\epsilon^2)+r_2(-(-1+n)V^2We^2+r_2(5(-1+n)V^2We^2-4(r_2-\delta)^2+\epsilon^2)))(\log(r_1)-\log(r_2)))\Big)+\epsilon^3$$
$$\times\cos 3\theta\Big(2\Big(63Qr_1^2(-80(r_2-\delta)^4-60(r_2-\delta)^2\epsilon^2-3\epsilon^4)+\pi(r_1-r_2)V(r_2-\delta)\times(2(-1+n)r_2^3(-2+3r_2)V^2We^2-2(-1$$
$$+n)r_1r_2^2(-8+9r_2)V^2We^2+4r_1^4(-16(-1+n)V^2We^2+328(r_2-\delta)^2+137\epsilon^2)+r_1^3(-4(4(-1+n)V^2We^2+r_2(67(-1+n)V^2We^2$$
$$+14(r_2-\delta)^2))+161r_2\epsilon^2)+r_1^2r_2(-92(-1+n)V^2We^2+r_2(-172(-1+n)V^2We^2-56(r_2-\delta)^2+161\epsilon^2))))$$
$$+3\pi r_1^2(-21(80(r_2-\delta)^4+60(r_2-\delta)^2\epsilon^2+3\epsilon^4)\phi^2\cos 4\pi(z-t)-4V(r_2-\delta)(4r_1^2(-(-1+n)V^2We^2+r_2(-9(-1+n)V^2We^2$$
$$+24(r_2-\delta)^2+16\epsilon^2))+4r_1r_2(-(-1+n)V^2We^2+r_2(-9(-1+n)V^2We^2+24(r_2-\delta)^2+16\epsilon^2))+r_2^2(-8(-1$$
$$+n)V^2We^2+r_2(-14(-1+n)V^2We^2+8(r_2-\delta)^2+17\epsilon^2)))(\log(r_1)-\log(r_2)))\Big)+12\pi r_1^2(3(r_2-\delta)(16(r_2-\delta)^6+168(r_2-\delta)^4\epsilon^2$$
$$+210(r_2-\delta)^2\epsilon^4+35\epsilon^6)\phi^2\cos 4\pi(z-t)+V(r_2^2(-8(-1+n)V^2We^2(r_2-\delta)^4+4(-6(-1+n)V^2We^2+r_2(5(-1+n)V^2We^2+14$$
$$\times(r_2-\delta)^2))(r_2-\delta)^2\epsilon^2+(-3(-1+n)V^2We^2+r_2(47(-1+n)V^2We^2+84(r_2-\delta)^2))\epsilon^4+7r_2\epsilon^6)+r_1^2(8(-(-1+n)V^2We^2$$
$$+2r_2(r_2-\delta)^2)(r_2-\delta)^4+4(-7(-1+n)V^2We^2+2r_2(6(-1+n)V^2We^2+29(r_2-\delta)^2))(r_2-\delta)^2\epsilon^2+2(-2(-1+n)V^2We^2$$
$$+3r_2(16(-1+n)V^2We^2+43(r_2-\delta)^2))\epsilon^4+19r_2\epsilon^6)+r_1r_2(8(-(-1+n)V^2We^2+2r_2(r_2-\delta)^2)(r_2-\delta)^4+4(-7(-1+n)V^2We^2$$
$$+2r_2(6(-1+n)V^2We^2+29(r_2-\delta)^2))(r_2-\delta)^2\epsilon^2+2(-2(-1+n)V^2We^2+3r_2(16(-1+n)V^2We^2+43(r_2-\delta)^2))\epsilon^4+19r_2\epsilon^6))$$
$$\times(\log(r_1)-\log(r_2)))+3r_1^2\epsilon^6$$
$$\times\cos 6\theta\Big(\pi\Big(-4r_1^3+9r_1^2r_2-5r_2^3\Big)V+84Q(r_2-\delta)+42\pi(r_2-\delta)\phi^2\times\cos 4\pi(z-t)+2\pi r_2\Big(r_1^2+r_1r_2+r_2^2\Big)V(-\log(r_1)+\log(r_2))\Big)\Big).$$

References

[1] Latham TW. Fluid motion in a peristaltic pump. Cambridge, MA: MIT; 1966.

[2] Yin CC, Fung YC. Peristaltic wave in circular cylindrical tubes. J Appl Mech 1969;36:579–87.

[3] Haroun MH. Non-linear peristaltic of a fourth grade fluid in an inclined asymmetric channel. Comput Mater Sci 2007;39:324–33.

[4] El Hakeem A, El Naby A, El Misery AEM, El Kareem MFA. Separation in the flow through peristaltic motion of a carreau fluid in uniform tube. Physica A 2004;343:1–14.

[5] Nadeem S, Akbar NS, Bibi N, Ashiq S. Influence of heat and mass transfer on peristaltic flow of a third order fluid in a diverging tube. Commun Nonlinear Sci Numer Simul 2010;15:2916–31.

[6] Nadeem S, Akram S. Influence of inclined magnetic field on peristaltic flow of a Jeffrey fluid with heat and mass transfer in an inclined symmetric or asymmetric channel. Asia-Pacific J Chem Eng 2012;7:33–44.

[7] Nadeem S, Akram S, Hayat T, Hendi AA. Peristaltic flow of a Carreau fluid in a rectangular duct. J Fluid Eng 2012;134:041201–7.

[8] Nadeem S, Akram S. Simulation of heat and mass transfer on peristaltic flow of hyperbolic tangent fluid in an asymmetric channel. Int J Numer Methods Fluids 2012;70:1475–93.

[9] Ellahi R, Riaz A, Nadeem S, Ali M. Peristaltic flow of Carreau fluid in a rectangular duct through a porous medium. Math Probl Eng 2012. http://dx.doi.org/10.1155/2012/329639.

[10] Nadeem S, Ghafoor A, Akram S. Mixed convective heat and Mass transfer on a peristaltic flow of a non-Newtonian fluid in a vertical asymmetric channel. Heat Transfer Asian Res 2012;41:613–33.

[11] Akram S, Nadeem S, Lee C. Influence of lateral walls on Peristaltic flow of a Jeffrey fluid in a rectangular duct with partial slip. Int J Appl Math 2012;14:449–63.

[12] Akbar NS, Nadeem S, Haq R, Khan ZH. Numerical solutions of magnetohydrodynamic boundary layer flow of tangent hyperbolic fluid towards a stretching sheet. Indian J Phys 2013;87:1121–4.

[13] Nadeem S, Haq R, Lee C. MHD flow of a Casson fluid over an exponentially shrinking sheet. Sci Iran 2012;19:1150–553.

[14] Nadeem S, Haq R, Khan ZH. Numerical study of MHD boundary layer flow of a Maxwell fluid past a stretching sheet in the presence of nanoparticles. J Taiwan Inst Chem Eng 2013. http://dx.doi.org/10.1016/j.jtice.2013.04.006.

[15] El Hakeem A, El Naby A, El Misery AEM, El Shamy II. Hydromagnetic flow of fluid with variable viscosity in a uniform tube with peristalsis. J Phys A 2003;368:535–47.

[16] Hariharan P, Seshadri V, Banerjee RK. Peristaltic transport of non-Newtonian fluid in a diverging tube with different wave forms. Math Comput Model 2008;48:998–1017.

[17] Ebaid A. A new numerical solution for the MHD peristaltic flow of a biofluid with variable viscosity in circular cylindrical tube via Adomian decomposition method. Phys Lett A 2008;372:5321–8.

[18] Srinivas S, Kothandapani M. The influence of heat and mass transfer on MHD peristaltic flow through a porous space with compliant walls. Appl Math Comput 2009;213:197–208.

[19] Mekheimer KS. Effect of the induced magnetic field on peristaltic flow of a couple stress fluid. Phys Lett A 2008;372:4271–8.

[20] Subba Reddy MV, Mishra M, Sreenadh S, Ramachandra Rao A. Influence of lateral walls on peristaltic flow in a rectangular duct. J Fluids Eng 2005;127:824–7.

[21] Srinivasacharya D, Srikanth D. Flow of micropolar fluid through catheterized artery – a mathematical model. Int J Biomath 2012;5:12.

[22] Mekheimer KhS, Abdelmaboud Y, Abdellateef AI. Peristaltic transport through an eccentric cylinders: mathematical model. Applied Bionics and Biomechanics 2013;10:19–27.

[23] Nadeem S, Riaz Arshad, Ellahi R, Mushtaq M. Series solutions of magnetohydrodynamic peristaltic flow of a Jeffrey fluid in eccentric cylinders. Appl Math Info Sci 2013;7:1441–9.
[24] He JH. Homotopy perturbation technique. Comput Meth Appl Mech Eng 1999;178:257–62.

Dr. Sohail Nadeem Associate Professor at Quaid-i-Azam University Islamabad. He is recipient of Razi-ud Din gold medal by Pakistan Academy of Sciences and Tamgha-i-Imtiaz by the President of Pakistan. He is young fellow of TWAS, Italy.

Mr. Arshad Riaz PhD Scholar in the department of Mathematics at International Islamic University, Islamabad under the supervision of Dr. Rahmat Ellahi. He obtained his MS degrees with distinction and published his research articles in internationally refereed journals.

Dr. R. Ellahi Fulbright Fellow in the University Of California Riverside, USA and also founder Chairperson of the Department of Mathematics and Statistics at IIUI, Pakistan. He has several awards and honors on his credit: Fulbright Fellow, Productive Scientist of Pakistan, Best University Teacher Award by higher education commission (HEC) Pakistan, Best Book Award, and Valued Reviewer Award by Elsevier. He is also an author of six books and editor of two international journals.

Dr. Noreen Sher Akbar Assistant Professor in DBS&H CEME, National University of Sciences and Technology, Islamabad Pakistan, She is an active researcher in the field of Applied Mathematics.